Polyphase ultramylonite development during shear zone evolution

Alexander D. Lusk[1,2], John P. Platt[2]

1 - Department of Geoscience, University of Wisconsin - Madison; 2 - Department of Earth Science, University of Southern California

alusk@wisc.edu

WISCONSIN UNIVERSITY OF WISCONSIN-MADISON

USC University of Southern California

CIG COMPUTATIONAL INFRASTRUCTURE for GEODYNAMICS

Study area:

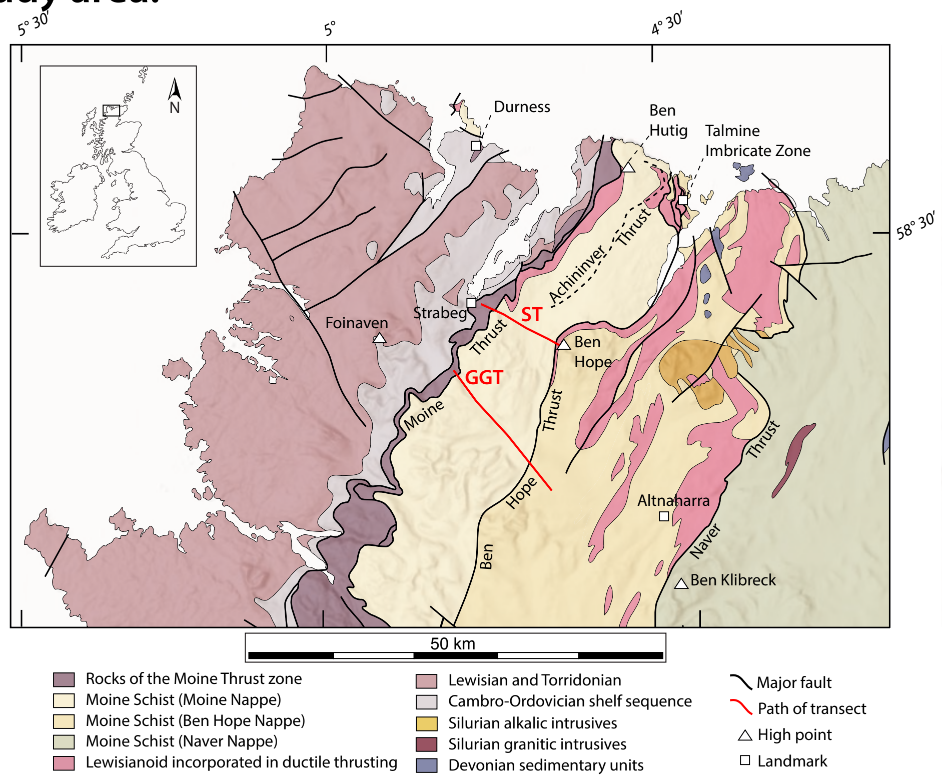

Location of transects across the Moine Nappe, northwest Scotland. Map modified from Ashley et al., 2015

Reconstructing the shear zone at depth:

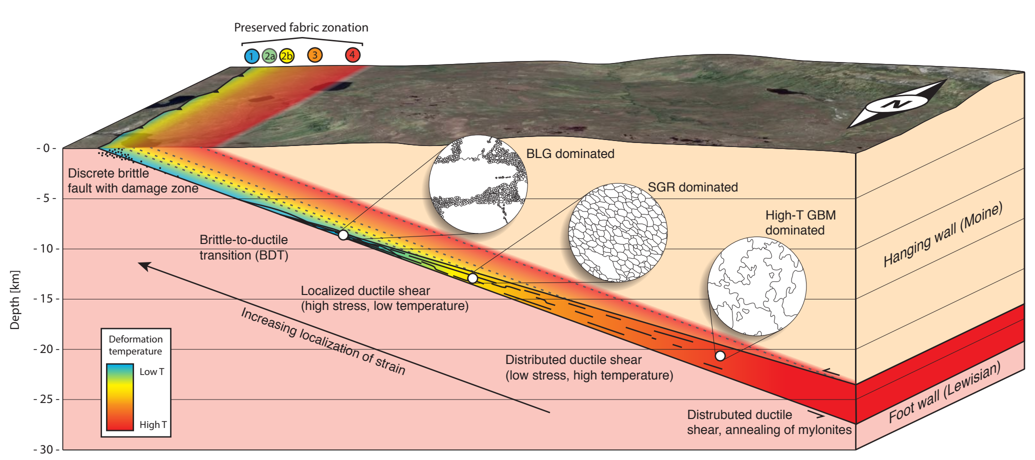

Schematic illustration of a generalized shear zone, modeled after constraints from the Moine shear zone (note that the overlying and underlying thrusts are ignored for this illustration). Localization of strain in the deeper regions results in rocks representative of different shear zones depths (and widths) uplifted piggy-back style along material lines (dashed). Continued movement along this zone will eventually give rise to a fabric zonation preserved at the surface. From Lusk and Platt (2020).

Fine-grained polyphase layer rheology:

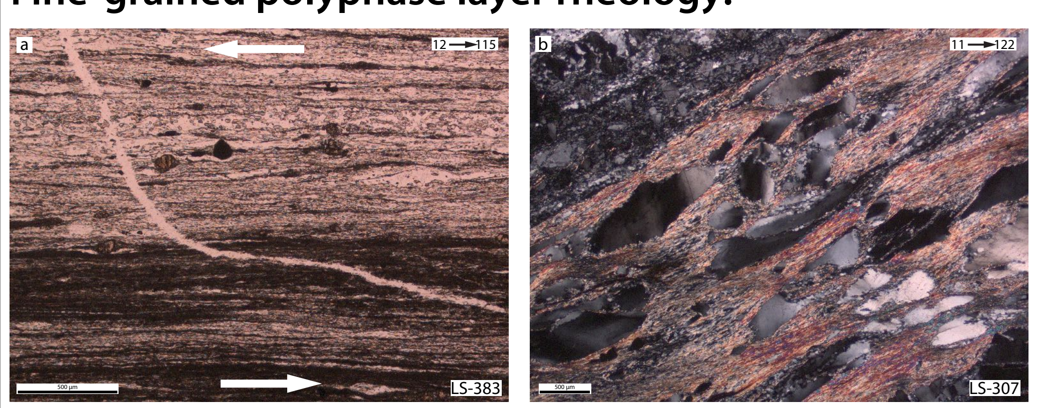

Interconnected polyphase fine-grained layers (a) and micaceous layers (b) are demonstrably weaker than the surrounding quartz. (a) a cross-cutting quartz vein shows more deflection in the poly-phase layer (lower portion) compared to the quartz-rich layer (upper portion). (b) a network of interconnected micas with variably-recrystallized quartz lozenges. (a) plane polarized light, (b) cross-polarized light.

* Deformation temperature and pressure determined by Ti-in-quartz (TitaniQ) and Si-in-white mica (see Lusk and Platt, 2020)

Strabeg transect (ST):

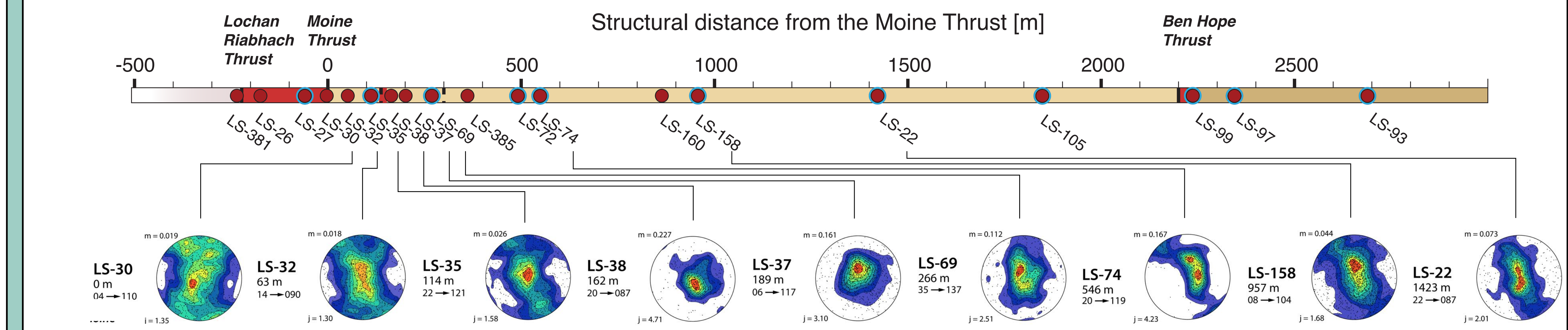

Quartz DRX mechanism(s):	BLG/SGR	SGR	SGR	SGR/GBM	SGR	SGR/GBM	GBM	GBM	GBM
Deformation temperature* [°C]:	N/D	N/D	356 (+34/-33)	N/D	N/D	382 (+49/-57)	354 (+20/-16)	374 (+34/-34)	431 (+23/-24)

← Fine-grained poly-phase layers present → ← Fine-grained poly-phase layers absent →

Glen Golly transect (GGT):

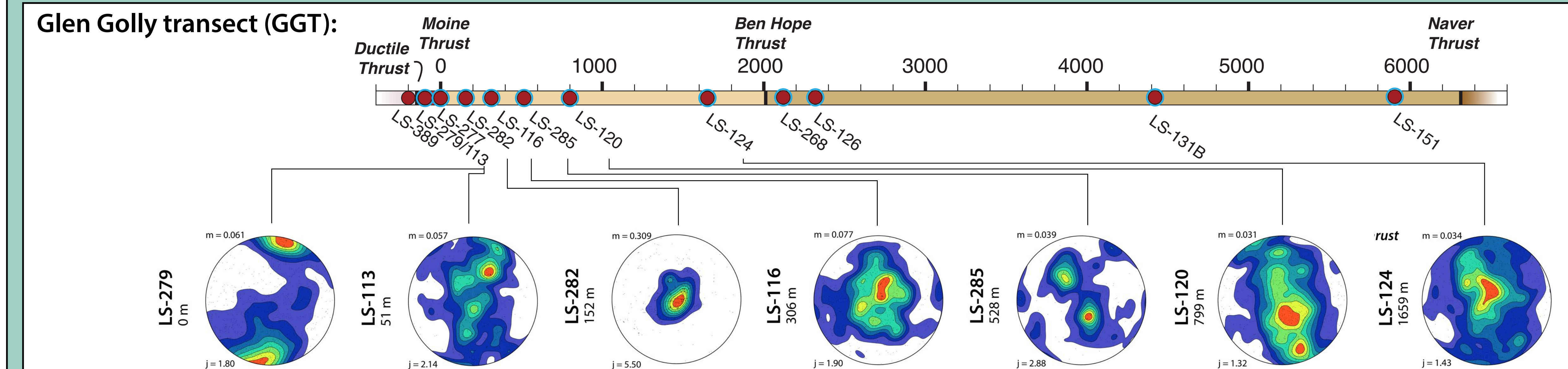

Quartz DRX mechanism:	BLG/SGR	SGR	GBM/SGR	GBM/SGR	GBM	GBM	GBM
Deformation temperature* [°C]:	310 (+17/-17)	328 (+16/-22)	344 (+22/-21)	321 (+19/-17)	N/D	371 (+19/-19)	401 (+20/-18)

← Fine-grained polyphase layers present → ← Fine-grained polyphase layers absent →

Fine-grained polyphase layer composition and microstructure:

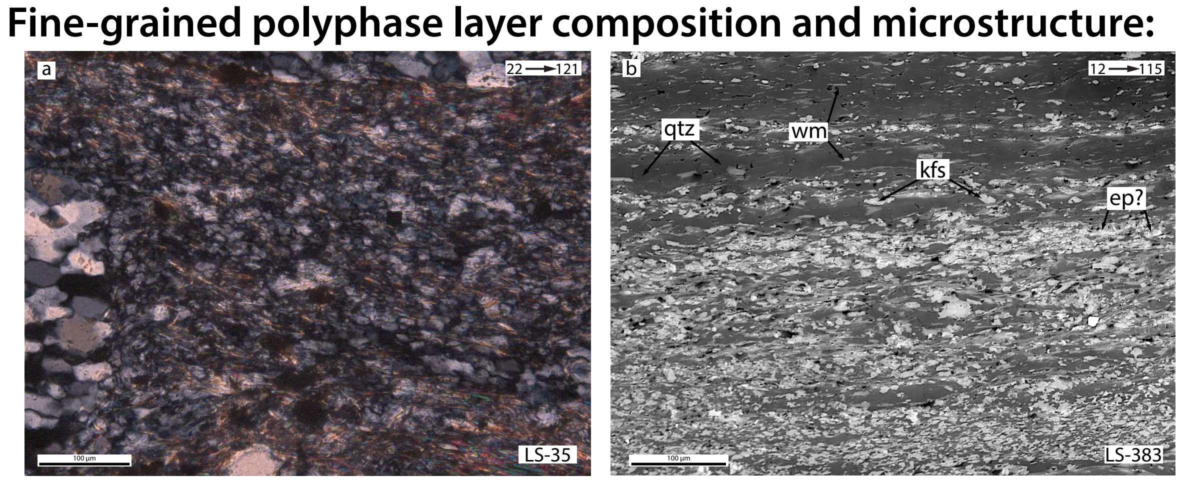

Cross-polarized optical (a) and backscatter electron (b) images of fine-grained polyphase aggregates. Both images show a mixing of quartz, micas, and feldspars into a fine-grained matrix distinct from that of pure quartz or matrix at higher structural levels. For (b), phases as follows: qtz – quartz; wm – white mica; kfs – potassic feldspar; ep? – possible epidote.

Mica comminution:

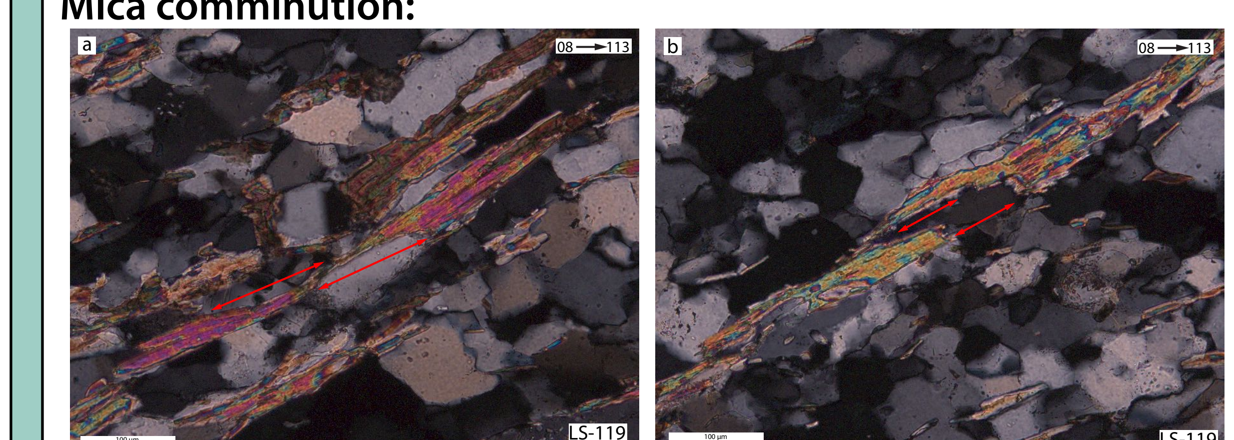

Mechanical separation of mica by fracture or dynamic recrystallization is a plausible mechanism to decrease the grain size and grow interconnected mica networks. (a) and (b) both illustrate possible mechanical separation parallel to red arrows based on the reconstructed fit of grain boundaries. Both images in cross-polarized light, foliation inclined towards ~060.

Microstructural characterization:

Strabeg transect

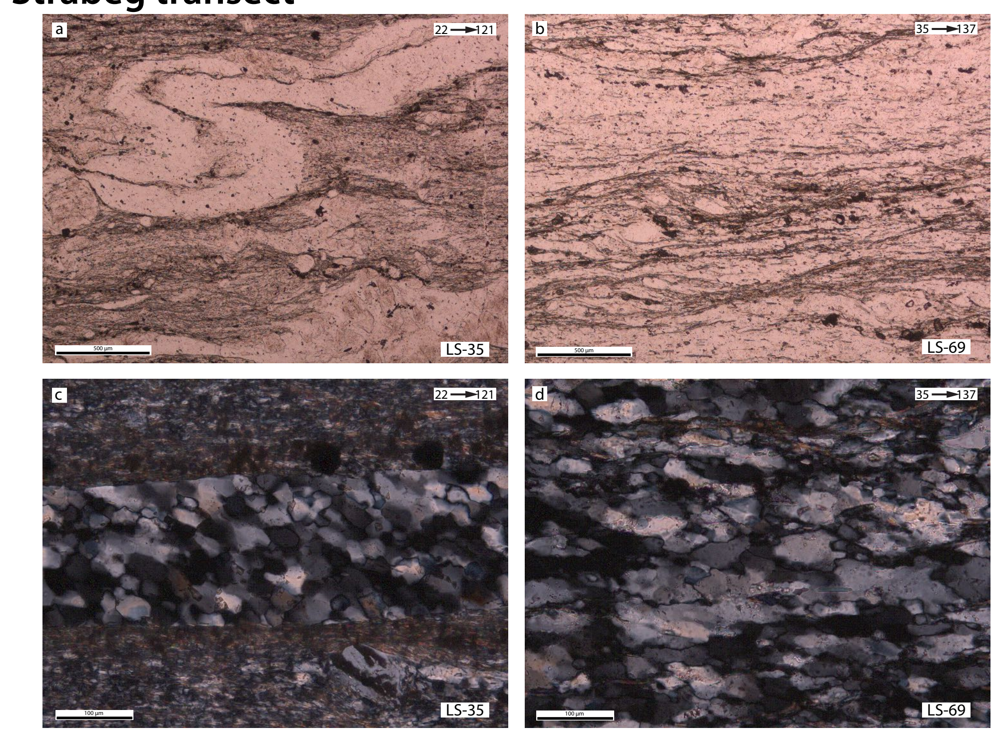

Glen Golly transect

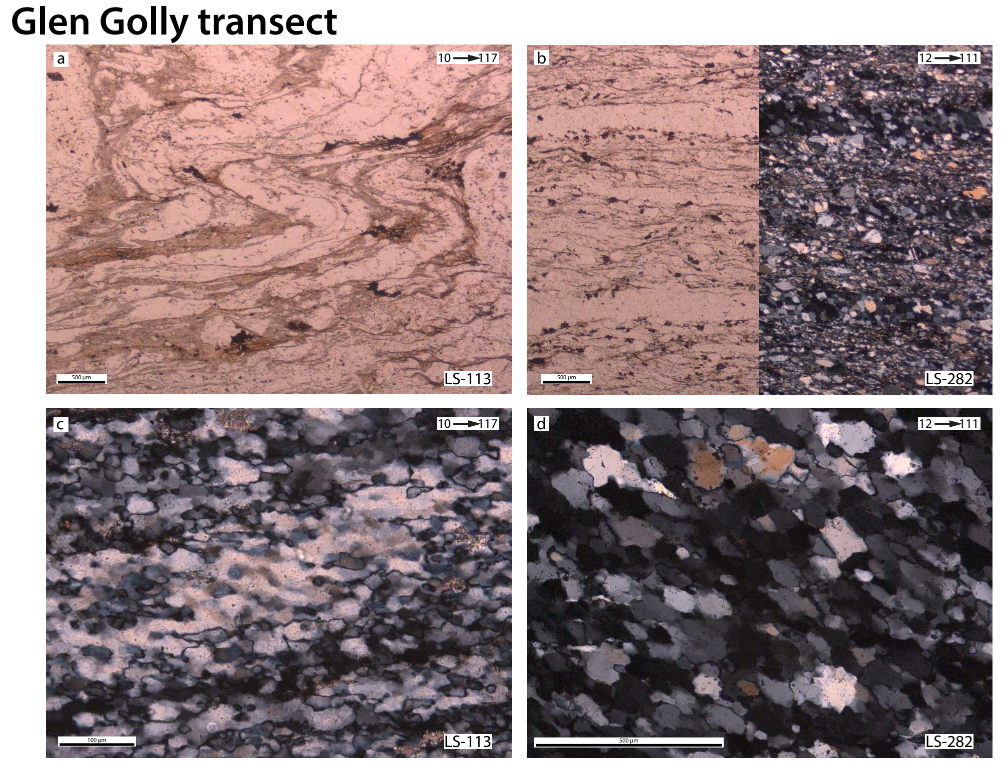

Comparison of fine-grained polyphase dominated microstructures at structurally lower levels (a) and coarser-grained quartz-dominated microstructures with interconnected micaceous layers at structurally higher levels (b) from the Strabeg Transect (top panel) and Glen Golly Transect (lower panel). Note buckle folding in (a) indicates that the quartz vein is stronger than the surrounding fine-grained polyphase matrix. In contrast, interconnected micaceous layers in (b) form shear bands, with no significant viscosity contrast observed in the matrix. This transition coincides with a change in dominant quartz recrystallization mechanism from high-T recrystallization by GBM/SGR (d), to recrystallization dominated by SGR (c).

Conclusions:

(1) Quartz CPOs record consistent transitions with changing temperature. Transitions are likely caused by changes in the active slip system(s), which we attribute to (a) a decrease in grain boundary mobility (and quartz recrystallization mechanism) due to lower temperature, and (b) finite strain.

(2) Quartz CPOs in the hanging wall of the Moine Thrust show evidence for inheritance of grain orientations from deeper regions, indicating incomplete transitions to the easy slip system at shallower levels.

(3) We postulate that transitions in easy slip system may transiently strengthen quartz aggregates, causing strain to become increasingly partitioned into phyllosilicate and polyphase layers. This partitioning could trigger the development of fine-grained polyphase interconnected weak networks, which likely deform by grain size sensitive mechanisms including diffusion-accommodated grain boundary sliding.